

Two Supramolecular Isomers of Molecular Squares and 1D Helical Chains with Alternating Right- and Left-Handed Chirality

Long Jiang, Tong-Bu Lu,* and Xiao-Long Feng

School of Chemistry and Chemical Engineering and Instrumentation Analysis & Research Center, Sun Yat-Sen University, Guangzhou 510275, China

Received April 24, 2005

The reaction of $[\text{Ni}(\alpha\text{-rac-L})](\text{ClO}_4)_2$ with $\text{K}_2[\text{Ni}(\text{CN})_4]$ gives a cyanide bridged [2+2] type of molecular square, $\{\text{cis-}[\text{Ni}(\text{f-rac-L})][\text{Ni}(\text{CN})_4]\}_2$ (**1**). By slightly changing the reaction conditions, the reaction of $[\text{Ni}(\alpha\text{-rac-L})](\text{ClO}_4)_2$ with KCN leads to a metastable compound, $\text{cis-}[\text{Ni}(\text{f-rac-L})(\text{CN})_2]$ (**2**), and an unexpected 1D helical chain, $\{\text{cis-}[\text{Ni}(\text{f-rac-L})][\text{Ni}(\text{CN})_4]\}_n$ (**3**). In **3**, the 1D helical chains are packed in an alternating right- and left-handed chirality due to the oppositely twisted arrangements of two adjacent $[\text{Ni}(\text{CN})_4]^{2-}$ anions. The metastable compound **2** can be converted to **3** in a $\text{CH}_3\text{CN}/\text{CH}_3\text{OH}$ solution. Compounds **1** and **3** are classified as supramolecular isomers, and isomer **3** can be considered to be formed by the ring-opening polymerization of the square precursor **1**. Magnetic susceptibility measurements of **1** and **3** show that the adjacent six-coordinated Ni(II) atoms are antiferromagnetically coupled through the bent $-\text{NC}-\text{Ni}-\text{CN}-$ bridges of the diamagnetic $[\text{Ni}(\text{CN})_4]^{2-}$ anions, with $g = 2.08$ and $J = -0.426 \text{ cm}^{-1}$ for **1** and $g = 2.08$ and $J = -0.278 \text{ cm}^{-1}$ for **3**. The correlation between the structures and the J values is discussed.

Introduction

Recently, increasing attention has been focused on supramolecular isomerism in the field of molecular architectures.^{1–4} For given building blocks, different arrangements of these building blocks can lead to the formation of a series of supramolecular isomers. The architectures of supramolecular

isomers are very sensitive to experimental conditions such as reaction temperature,² template molecules,^{3a} solvents,^{3b,3c} and so forth. Chen et al.^{3a} reported three supramolecular isomers of a one-dimensional (1D) zigzag chain and two discrete octagonal and decagonal molecular rings by the reactions of $\text{Cu}(\text{NO}_3)_2$ with 2-methylimidazolate in the presence of either methanol, toluene, or *p*-xylene template molecules, respectively. They^{3b} also described two solvent polarity-induced supramolecular isomers of one triple-stranded helical and one zigzag chainlike structure. Zaworotko et al.^{1c} demonstrated that the one-pot reaction of 5-nitro-1,3-benzenedicarboxylic acid and Cu(II) ions gave two supramolecular isomers of a discrete molecular hexagon and a polymeric zigzag chain. The conversion process from the discrete closed structures to the polymeric one can be described as ring-opening polymerization^{4a–4c} or ring-opening isomerism.^{4d} Though ring-opening polymerization is common in organic polymers,⁵ only a few examples have been reported in coordination polymers.^{1c,3a,4}

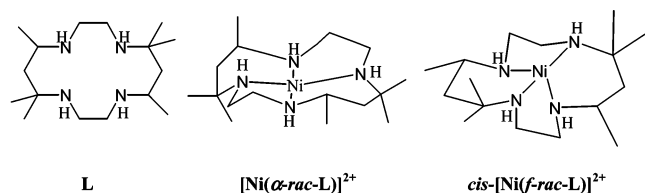
Nickel complexes of the macrocyclic ligand 5,5,7,12,12-,14-hexamethyl-1,4,8,11-tetraazacyclotetradecane (L, see Scheme 1) exhibit several conformational isomers, depending on the configurations of the two asymmetric carbon atoms

(5) *Ring Opening Polymerization*; Ivin, K. J., Saegusa, T., Eds.; Elsevier: New York, 1984.

* Author to whom correspondence should be addressed. Tel.: +86-20-84112921. E-mail: cesltb@zsu.edu.cn

- (1) (a) Hennigar, T. L.; MacQuarrie, D. C.; Losier, P.; Rogers, R. D.; Zaworotko, M. J. *Angew. Chem. Int. Ed. Engl.* **1997**, *36*, 972. (b) Moulton, B.; Zaworotko, M. J. *Chem. Rev.* **2001**, *101*, 1629. (c) Abourahma, H.; Moulton, B.; Kravtsov, V.; Zaworotko, M. J. *J. Am. Chem. Soc.* **2002**, *124*, 9990. (d) Ma, S. H.; Rudkevich, D. M.; Rebek, J. *Angew. Chem., Int. Ed.* **1999**, *38*, 2600. (e) Bernstein, J.; Davey, R. J.; Henck, J. O. *Angew. Chem., Int. Ed.* **1999**, *38*, 3440. (f) Masciocchi, N.; Bruni, S.; Cariati, E.; Cariati, F.; Galli, S.; Sironi, A. *Inorg. Chem.* **2001**, *40*, 5897. (g) Zhang, J. P.; Lin, Y. Y.; Huang, X. C.; Chen, X. M. *Chem. Commun.* **2005**, 1258.
- (2) (a) Masaoka, S.; Tanaka, D.; Nakanishi, Y.; Kitagawa, S. *Angew. Chem., Int. Ed.* **2004**, *43*, 2530. (b) Tong, M. L.; Hu, S.; Wang, J.; Kitagawa, S.; Ng, S. W. *Cryst. Growth Des.* **2005**, *5*, 837.
- (3) (a) Huang, X. C.; Zhang, J. P.; Chen, X. M. *J. Am. Chem. Soc.* **2004**, *126*, 13218. (b) Huang, X. C.; Zhang, J. P.; Lin, Y. Y.; Chen, X. M. *Chem. Commun.* **2005**, 2232. (c) Soldatov, D. V.; Ripmeester, J. A.; Shergina, S. I.; Sokolov, I. E.; Zanina, A. S.; Gromilov, S. A.; Dyadin, Y. A. *J. Am. Chem. Soc.* **1999**, *121*, 4179.
- (4) (a) Lozano, E.; Nieuwenhuyzen, M.; James, S. L. *Chem.—Eur. J.* **2001**, *7*, 2644. (b) Qin, Z. Q.; Jennings, M. C.; Puddephatt, R. J. *Chem.—Eur. J.* **2002**, *8*, 735. (c) Brandys, M.-C.; Puddephatt, R. J. *J. Am. Chem. Soc.* **2002**, *124*, 3946. (d) Su, C. Y.; Goforth, A. M.; Smith, M. D.; zur Loye, H.-C. *Inorg. Chem.* **2003**, *42*, 5685.

Scheme 1



and the four asymmetric nitrogen atoms. In our previous work,⁶ we described how to control the experimental conditions to obtain six-coordinated nickel(II) complexes with defined cis or trans configurations by the reaction of $[\text{Ni}(\alpha\text{-rac-L})](\text{ClO}_4)_2$ or $[\text{Ni}(\beta'\text{-rac-L})](\text{ClO}_4)_2$ cations with different bridging ligands. Interestingly, by carefully controlling the experimental conditions, we were able to construct two cyanide bridged supramolecular isomers of one molecular square, $\{[\text{Ni}(\alpha\text{-rac-L})][\text{Ni}(\text{CN})_4]\}_2$ (**1**), and one 1D helical chain, $\{[\text{Ni}(\alpha\text{-rac-L})][\text{Ni}(\text{CN})_4]\}_n$ (**3**), in which **3** can be considered to be formed by the ring-opening polymerization of the square precursor **1**. To the best of our knowledge, similar molecular squares and 1D helical chains have not been reported in complexes of $[\text{Ni}(\text{CN})_4]^{2-}$ with macrocyclic metal compounds.

Experimental Section

Materials and General Methods. The macrocyclic ligand (**L**) and its nickel(II) complex $[\text{Ni}(\alpha\text{-rac-L})](\text{ClO}_4)_2$ were prepared according to the previously reported method.⁶ $\text{K}_2\text{Ni}(\text{CN})_4 \cdot 2\text{H}_2\text{O}$ was prepared according to the literature method.⁷ All of the other chemicals are commercially available and were used without further purification. Elemental analyses were determined using an Elementar Vario EL elemental analyzer. The IR spectra were recorded in the 400–4000 cm^{-1} region using KBr pellets and a Bruker EQUINOX 55 spectrometer. ESI-MS spectra were obtained using a Shimadzu LCMS-2010A mass spectrometer. Magnetic susceptibility data were collected in the 2–300 K temperature range with a Quantum Design SQUID Magnetometer MPMS XL-7 with an applied field of 1 T. A correction was made for diamagnetic contributions prior to data analysis.

$\{cis\text{-}[\text{Ni}(f\text{-rac-L})][\text{Ni}(\text{CN})_4]\}_2$, **1.** A water solution (20 mL) of $\text{K}_2\text{Ni}(\text{CN})_4 \cdot 2\text{H}_2\text{O}$ (0.111 g, 0.4 mmol) was layered with an acetonitrile solution (20 mL) of $[\text{Ni}(\alpha\text{-rac-L})](\text{ClO}_4)_2$ (0.216 g, 0.4 mmol). After about 2 weeks, block-shaped purple crystals of **1**· $2\text{H}_2\text{O}$ formed from the solution. The crystals were collected, washed with water and methanol, and dried in the air. Yield: 0.214 g, 51%. Anal. Calcd for $\text{C}_{40}\text{H}_{76}\text{N}_{16}\text{Ni}_4\text{O}_2$ (**1**· $2\text{H}_2\text{O}$): C, 45.85; H, 7.25; N, 21.39. Found: C, 45.98; H, 7.12; N, 21.41%. IR (KBr): ν_{CN} 2162 (coordinated) and 2126 (uncoordinated) cm^{-1} .

$cis\text{-}[\text{Ni}(f\text{-rac-L})(\text{CN})_2]$, **2.** A solution of KCN (0.026 g, 0.4 mmol) in 10 mL of cold water was added to a solution of $[\text{Ni}(\alpha\text{-rac-L})](\text{ClO}_4)_2$ (0.108 g, 0.2 mmol) in 20 mL of cold acetonitrile. The resulting solution was filtered, and the filtrate was evaporated at a low temperature to give plate-shaped purple crystals of **2**· $2\text{H}_2\text{O}$ within about 1 week. The crystals were filtered, washed with water and acetonitrile, and dried in the air. Yield: 0.060 g, 69%. Anal. Calcd for $\text{C}_{18}\text{H}_{40}\text{N}_6\text{NiO}_2$ (**2**· $2\text{H}_2\text{O}$): C, 50.13; H, 9.35; N, 19.49. Found: C, 50.46; H, 8.90; N, 19.45%. IR (KBr): ν_{CN} 2094 cm^{-1} .

$\{cis\text{-}[\text{Ni}(f\text{-rac-L})][\text{Ni}(\text{CN})_4]\}_n$, **3.** A solution of KCN (0.026 g, 0.4 mmol) in 20 mL of cold water was added to a solution of $[\text{Ni}(\alpha\text{-rac-L})](\text{ClO}_4)_2$ (0.108 g, 0.2 mmol) in 20 mL of cold acetonitrile. The resulting solution was filtered, and the filtrate was evaporated at a low temperature to give prism-shaped violet crystals of **3**· $(4.5\text{H}_2\text{O})_n$ within about 1 month. The crystals were filtered, washed with water and methanol, and dried in the air. Yield: 0.041 g, 70%. Anal. Calcd for $\text{C}_{20}\text{H}_{44}\text{N}_8\text{Ni}_2\text{O}_4$ (**3**· $4\text{H}_2\text{O}$): C, 41.56; H, 7.61; N, 19.39. Found: C, 41.67; H, 7.60; N, 19.45%. IR (KBr): ν_{CN} 2158 (coordinated) and 2127 (uncoordinated) cm^{-1} .

The crystals of **3**· $(4.5\text{H}_2\text{O})_n$ can also be obtained by dissolving **2** in a mixture solution of acetonitrile and methanol (1:1) and evaporating slowly at room temperature.

X-ray Crystallography. Single-crystal data of **1**· $2\text{H}_2\text{O}$, **2**· $2\text{H}_2\text{O}$, and **3**· $(4.5\text{H}_2\text{O})_n$ were collected at 293(2) K on a Bruker Smart 1000 CCD diffractometer with Mo K α radiation ($\lambda = 0.71073$ Å). All empirical absorption corrections were applied by using the SADABS program.⁸ The structures were solved using direct methods, which yielded the positions of all non-hydrogen atoms. These were refined, first, isotropically and, then, anisotropically. All the hydrogen atoms of the ligands were placed in calculated positions with fixed isotropic thermal parameters and included in the structure factor calculations in the final stage of full-matrix least-squares refinement. The hydrogen atoms of the water molecules were located in the difference Fourier map and refined isotropically; the O–H distances involving the water molecules were refined with a DFIX restraint of 0.86 Å. All calculations were performed using the SHELXTL system of computer programs.⁹ The crystallographic data for **1**–**3** are summarized in Table 1. The selected bond lengths and angles for **1**–**3** are listed in Table 2.

Results and Discussion

Synthesis and Solution Studies. The $[\text{Ni}(\text{CN})_4]^{2-}$ anion usually forms 1D linear chains with *trans*-Ni(II) tetradentate macrocyclic complexes.¹⁰ In reactions with *cis*-octahedral Ni(II) tetradentate macrocyclic complexes, $[\text{Ni}(\text{CN})_4]^{2-}$ can construct six possible supramolecular isomers (see Scheme 2): a [2+2] molecular square (isomer **1**), a [4+4] molecular square (isomer **2**), 1D zigzag chains (isomers **4** and **5**), and 1D helical chains (isomers **3** and **6**). However, considering the repulsive interactions between the two terminal nitrogen atoms of two uncoordinated cyano groups, isomers **4** and **5** with 1D zigzag chainlike structures cannot be formed. The two adjacent $[\text{Ni}(\text{CN})_4]^{2-}$ planes should be twisted to avoid the repulsive interactions between the two uncoordinated cyano groups, and this leads to the formation of isomers **3** and **6** with 1D helical chainlike structures. Therefore, only four possible supramolecular isomers (**1**, **2**, **3**, and **6**) could be constructed by using *cis*- $[\text{Ni}(f\text{-rac-L})]^{2+}$ and $[\text{Ni}(\text{CN})_4]^{2-}$ building blocks.

Two supramolecular isomers (isomers **1** and **3**) were successfully synthesized in this study by using different

(8) Sheldrick, G. M. *SADABS, Program for Empirical Absorption Correction of Area Detector Data*; University of Göttingen: Göttingen, Germany, 1996.

(9) Sheldrick, G. M. *SHELXS 97, Program for Crystal Structure Refinement*; University of Göttingen, Göttingen, Germany, 1997.

(10) (a) Gainsford, G. J.; Curtis, N. F. *Aust. J. Chem.* **1984**, *37*, 1799. (b) Kou, H. Z.; Si, S. F.; Gao, S.; Liao, D. Z.; Jiang, Z. H.; Yan, S. P.; Fan, Y. G.; Wang, G. L. *Eur. J. Inorg. Chem.* **2002**, 699. (c) Kou, H. Z.; Liao, D. Z.; Jiang, Z. H.; Yan, S. P.; Wu, Q. J.; Gao, S.; Wang, G. L. *Inorg. Chem. Commun.* **2000**, *3*, 151.

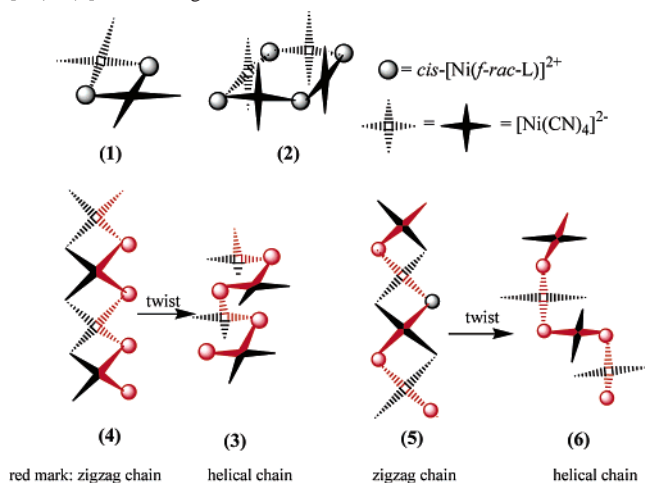
(6) Jiang, L.; Feng, X. L.; Lu, T. B. *Cryst. Growth Des.* **2005**, *5*, 1469.

(7) Ferneliuss, W. C. *Inorganic Synthesis*; McGraw-Hill: New York, 1946; Vol. II, p 227.

Table 1. Crystallographic Data for 1–3

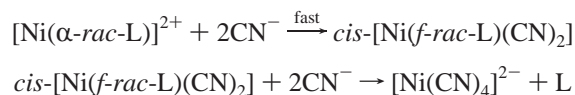
compound	1·2H ₂ O	2·2H ₂ O	3·(4.5H ₂ O) _n
formula	C ₄₀ H ₇₆ N ₁₆ Ni ₄ O ₂	C ₁₈ H ₄₀ N ₆ NiO ₂	C ₂₀ H ₄₅ N ₈ Ni ₂ O _{4.5}
fw	1048.01	431.27	587.06
cryst size (mm)	0.36 × 0.35 × 0.27	0.50 × 0.32 × 0.12	0.48 × 0.33 × 0.27
cryst syst	monoclinic	orthorhombic	monoclinic
space group	<i>P</i> 2 ₁ / <i>c</i>	<i>P</i> 2 ₁ 2 ₁ 2 ₁	<i>P</i> 2 ₁ / <i>c</i>
<i>a</i> /Å	16.330(12)	8.636(3)	9.962(2)
<i>b</i> /Å	22.908(16)	13.335(4)	10.368(2)
<i>c</i> /Å	13.866(10)	19.179(6)	28.389(6)
β/deg	90.317(13)	90	91.548(4)
vol/Å ³	5187(6)	2209(1)	2931(1)
<i>Z</i>	4	4	4
<i>D_c</i> /g cm ⁻³	1.342	1.297	1.330
μ/mm ⁻¹	1.478	0.903	1.324
reflns collected	31 541	12 090	14 094
unique reflns (<i>R</i> _{int})	11 305 (0.0612)	4792 (0.0334)	5731 (0.0345)
params	578	262	322
<i>S</i> on <i>F</i> ²	1.051	1.085	1.081
<i>R</i> ₁ , ^a <i>wR</i> ₂ ^b [<i>I</i> > 2σ(<i>I</i>)]	0.0659, 0.1574	0.0402, 0.0981	0.0373, 0.0903
<i>R</i> ₁ , ^a <i>wR</i> ₂ ^b (all data)	0.1231, 0.1942	0.0625, 0.1082	0.0652, 0.1101

^a $R_1 = \sum ||F_o| - |F_c|| / \sum |F_o|$. ^b $wR_2 = [\sum [w(F_o^2 - F_c^2)^2] / \sum w(F_o^2)^2]^{1/2}$. Weighting: **1**, $w = 1/[\sigma^2(F_o^2) + (0.0928P)^2 + 7.2634P]$; **2**, $w = 1/[\sigma^2(F_o^2) + (0.0557P)^2 + 0.0000P]$; **3**, $w = 1/[\sigma^2(F_o^2) + (0.0575P)^2 + 0.0000P]$; where $P = [(F_o^2) + 2F_c^2]/3$.

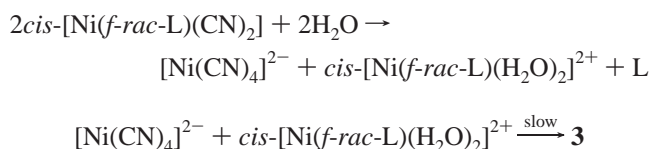
Scheme 2. Six Possible Arrangements of *cis*-[Ni(*f*-*rac*-L)]²⁺ and [Ni(CN)₄]²⁻ Building Blocks

methods of preparation. Isomer **1** could be obtained by carefully layering a water solution of K₂[Ni(CN)₄] with an acetonitrile solution of [Ni(α-*rac*-L)](ClO₄)₂. Under these reaction conditions, the neutral compound of isomer **1** was isolated quickly from the solution as a result of its low solubility once the [Ni(α-*rac*-L)]²⁺ and [Ni(CN)₄]²⁻ building blocks met together.

Interestingly, the reaction of [Ni(α-*rac*-L)](ClO₄)₂ and KCN in a mixture of 10 mL of water and 20 mL of acetonitrile led to the metastable compound **2** within 1 week. The same reaction in 20 mL of water and 20 mL of acetonitrile unexpectedly yielded compound **3** within 1 month. In the latter case, the metastable compound **2** formed but did not crystallize out from the dilute solution, and it was slowly converted to the less soluble compound **3**. During the formation of **3**, the following reactions occurred:



or



in which a thermodynamically favorable [Ni(CN)₄]²⁻ anion was formed from **2**, and [Ni(CN)₄]²⁻ then reacts slowly with [Ni(α-*rac*-L)]²⁺ to form **3**. In addition, compound **2** itself could be converted to **3** in an acetonitrile/methanol solution. The results of the ESI-MS spectra of **2** (see the Supporting Information) indicate that **2** was converted to several new species in the acetonitrile/methanol/water (1:1:1) solution, the main species corresponding to [NiL(CN)(H₂O)]⁺, [NiL]⁺, [HL]⁺, {[Ni(H₂L)][Ni(CN)₄]}²⁺, {[Ni(HL)]₂[Ni(CN)₄]}⁴⁺, [Ni(H₂L)(CN)₂(H₂O)]²⁺, and [(Ni(HL)(CN))]²⁺ {NiL = *cis*-[Ni(*f*-*rac*-L)]²⁺ (six-coordinated) or [Ni(α-*rac*-L)]²⁺ (four-coordinated)}, indicating that the coordinated CN⁻ anions exchange quickly with water molecules in solution. The intermediate species of {[Ni(H₂L)][Ni(CN)₄]}²⁺ and {[Ni(HL)]₂[Ni(CN)₄]}⁴⁺ correspond to oligomers of **3**, and these oligomers aggregate in solution to form the insoluble compound **3** with 1D helical chain structures. Indeed, after the solution was left for 2 days, the species {[Ni(H₂L)][Ni(CN)₄]}²⁺, {[Ni(HL)]₂[Ni(CN)₄]}⁴⁺, and [Ni(H₂L)(CN)₂(H₂O)]²⁺ disappeared, and the intensities of the peaks corresponding to [NiL(CN)(H₂O)]⁺, [NiL]⁺, and [(Ni(HL)(CN))]²⁺ decreased, while the intensity of the peak corresponding to [HL]⁺ had increased. This clearly demonstrates that compound **2** is slowly converted to **3** in solution and the free macrocyclic ligand L is produced.

We believe that isomer **1** could also be converted to isomer **3** since the ESI-MS spectrum of isomer **1** in a water/acetonitrile (1:1) solution shows three main species of [NiL(CN)(H₂O)]⁺, [NiL]⁺, and {[Ni(HL)]₂[Ni(CN)₄]}⁴⁺, which are disintegrated from isomer **1**. Unfortunately, we cannot find suitable solvents to dissolve isomer **1** since it is only slightly soluble in common solvents. We are still trying to

Table 2. Selected Bond Distances (Å) and Angles (deg) for **1–3**^a

1					
Ni(1)–N(1)	2.187(4)	Ni(1)–N(2)	2.126(3)	Ni(1)–N(3)	2.165(4)
Ni(1)–N(4)	2.106(4)	Ni(1)–N(5)	2.100(4)	Ni(1)–N(6)	2.121(3)
Ni(2)–C(17)	1.862(4)	Ni(2)–C(18)	1.863(4)	Ni(2)–C(19)	1.849(5)
Ni(2)–C(20)	1.881(5)	C(17)–N(5)	1.137(5)	C(18)–N(6)#1	1.149(5)
C(19)–N(8)	1.137(8)	C(20)–N(7)	1.139(6)		
Ni(3)–N(9)	2.146(4)	Ni(3)–N(10)	2.099(4)	Ni(3)–N(11)	2.161(4)
Ni(3)–N(12)	2.137(4)	Ni(3)–N(13)	2.107(4)	Ni(3)–N(14)	2.108(4)
Ni(4)–C(37)	1.879(5)	Ni(4)–C(38)#2	1.840(4)	Ni(4)–C(39)	1.850(6)
Ni(4)–C(40)	1.861(5)	C(37)–N(14)	1.117(6)	C(38)–N(13)	1.150(5)
C(39)–N(15)	1.167(9)	C(40)–N(16)	1.129(7)		
N(5)–Ni(1)–N(4)	166.35(15)	N(5)–Ni(1)–N(6)	84.65(13)		
N(4)–Ni(1)–N(6)	90.30(14)	N(5)–Ni(1)–N(2)	89.46(13)		
N(4)–Ni(1)–N(2)	97.69(14)	N(6)–Ni(1)–N(2)	167.88(14)		
N(5)–Ni(1)–N(3)	108.45(15)	N(4)–Ni(1)–N(3)	83.69(16)		
N(6)–Ni(1)–N(3)	85.32(15)	N(2)–Ni(1)–N(3)	86.51(15)		
N(5)–Ni(1)–N(1)	82.40(15)	N(4)–Ni(1)–N(1)	86.92(15)		
N(6)–Ni(1)–N(1)	106.52(14)	N(2)–Ni(1)–N(1)	83.10(13)		
N(3)–Ni(1)–N(1)	164.94(15)	C(19)–Ni(2)–C(17)	177.9(2)		
C(19)–Ni(2)–C(18)	90.9(2)	C(17)–Ni(2)–C(18)	90.46(16)		
C(19)–Ni(2)–C(20)	89.0(2)	C(17)–Ni(2)–C(20)	89.79(16)		
C(18)–Ni(2)–C(20)	176.1(2)	N(10)–Ni(3)–N(13)	168.40(16)		
N(10)–Ni(3)–N(14)	89.20(15)	N(13)–Ni(3)–N(14)	85.39(15)		
N(10)–Ni(3)–N(12)	99.85(16)	N(13)–Ni(3)–N(12)	87.22(15)		
N(14)–Ni(3)–N(12)	167.28(15)	N(10)–Ni(3)–N(9)	83.53(15)		
N(13)–Ni(3)–N(9)	106.08(14)	N(14)–Ni(3)–N(9)	84.35(15)		
N(12)–Ni(3)–N(9)	87.79(15)	N(10)–Ni(3)–N(11)	88.40(16)		
N(13)–Ni(3)–N(11)	83.05(16)	N(14)–Ni(3)–N(11)	104.47(16)		
N(12)–Ni(3)–N(11)	84.84(15)	N(9)–Ni(3)–N(11)	168.00(15)		
C(38)#2–Ni(4)–C(39)	173.8(3)	C(38)#2–Ni(4)–C(40)	89.9(2)		
C(39)–Ni(4)–C(40)	93.3(2)	C(38)#2–Ni(4)–C(37)	89.64(19)		
C(39)–Ni(4)–C(37)	86.8(2)	C(40)–Ni(4)–C(37)	176.6(2)		
2					
Ni(1)–C(17)	2.084(4)	Ni(1)–C(18)	2.085(4)	Ni(1)–N(2)	2.167(3)
Ni(1)–N(4)	2.199(3)	Ni(1)–N(1)	2.211(3)	Ni(1)–N(3)	2.211(3)
C(17)–N(5)	1.122(5)	C(18)–N(6)	1.143(5)		
C(17)–Ni(1)–C(18)	89.06(15)	C(17)–Ni(1)–N(2)	88.43(13)		
C(18)–Ni(1)–N(2)	170.29(13)	C(17)–Ni(1)–N(4)	170.10(12)		
C(18)–Ni(1)–N(4)	88.72(12)	N(2)–Ni(1)–N(4)	95.30(12)		
C(17)–Ni(1)–N(1)	86.28(13)	C(18)–Ni(1)–N(1)	106.49(12)		
N(2)–Ni(1)–N(1)	82.70(11)	N(4)–Ni(1)–N(1)	85.11(10)		
C(17)–Ni(1)–N(3)	107.33(13)	C(18)–Ni(1)–N(3)	86.65(12)		
N(2)–Ni(1)–N(3)	85.15(11)	N(4)–Ni(1)–N(3)	82.17(10)		
N(1)–Ni(1)–N(3)	161.49(11)				
3					
Ni(1)–N(1)	2.159(3)	Ni(1)–N(2)	2.121(2)	Ni(1)–N(3)	2.155(3)
Ni(1)–N(4)	2.139(3)	Ni(1)–N(5)	2.093(3)	Ni(1)–N(8)	2.089(3)
Ni(2)–C(17)	1.859(3)	Ni(2)–C(18)	1.865(4)	Ni(2)–C(19)	1.852(4)
Ni(2)–C(20)	1.863(3)	C(17)–N(5)	1.138(4)	C(18)–N(6)	1.136(5)
C(19)–N(7)	1.134(5)	C(20)–N(8)#1	1.141(4)		
N(8)–Ni(1)–N(5)	86.34(11)	N(8)–Ni(1)–N(2)	88.29(10)		
N(5)–Ni(1)–N(2)	168.75(10)	N(8)–Ni(1)–N(4)	169.42(11)		
N(5)–Ni(1)–N(4)	88.82(11)	N(2)–Ni(1)–N(4)	98.03(10)		
N(8)–Ni(1)–N(3)	104.82(10)	N(5)–Ni(1)–N(3)	84.07(10)		
N(2)–Ni(1)–N(3)	87.77(10)	N(4)–Ni(1)–N(3)	84.00(10)		
N(8)–Ni(1)–N(1)	85.16(11)	N(5)–Ni(1)–N(1)	105.25(11)		
N(2)–Ni(1)–N(1)	84.11(10)	N(4)–Ni(1)–N(1)	87.05(10)		
N(3)–Ni(1)–N(1)	166.96(10)	C(19)–Ni(2)–C(17)	174.32(18)		
C(19)–Ni(2)–C(20)	87.98(16)	C(17)–Ni(2)–C(20)	90.09(13)		
C(19)–Ni(2)–C(18)	89.85(18)	C(17)–Ni(2)–C(18)	91.95(15)		
C(20)–Ni(2)–C(18)	177.46(15)				
O(1)···N(7)	2.805(5)	O(1)–H(1D)···N(7)	169.7		
O(1)···O(2)#4	2.719(4)	O(1)–H(1E)···O(2)#4	159.8		
O(2)···O(3)#5	2.765(6)	O(2)–H(2D)···O(3)#5	165.7		
O(2)···O(1)#6	2.832(5)	O(2)–H(2E)···O(1)#6	158.7		
O(3)···N(6)	2.951(5)	O(3)–H(3D)···N(6)	170.9		

^a Symmetry transformations used to generate equivalent atoms: Isomer **1**: #1 $-x + 2, -y + 1, -z$; #2 $-x + 3, -y + 1, -z - 2$. Isomer **3**: #1 $-x, y + 1/2, -z + 1/2$; #4 $x, -y + 3/2, z - 1/2$; #5 $-x + 1, y + 1/2, -z + 1/2$; #6 $-x + 1, y - 1/2, -z + 1/2$; #7 $x, y, z - 1$.

seek suitable solvents to study the conversion from isomer **1** to isomer **3**. However, it appears impossible to convert

isomer **3** to isomer **1** since **3** is totally insoluble in common solvents.

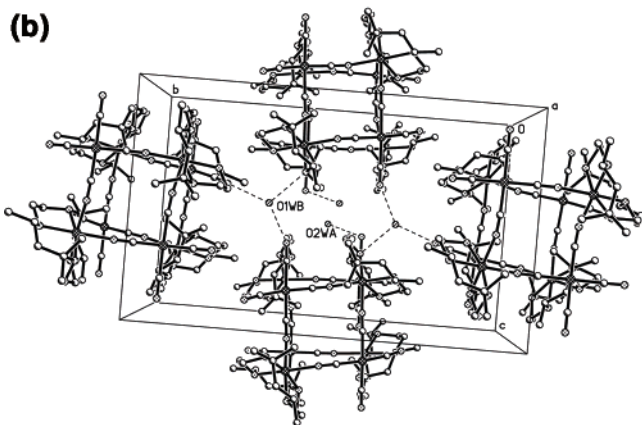
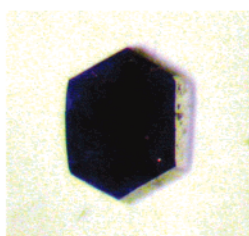
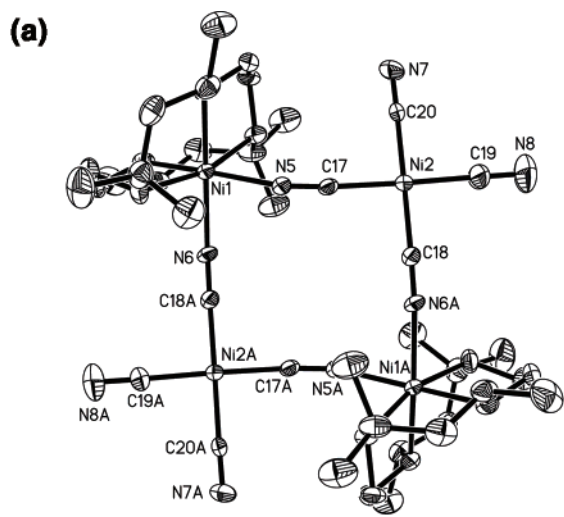


Figure 1. (a) ORTEP drawing of isomer **1** (thermal ellipsoids are drawn at the 30% level; top) and a photograph of a single crystal of isomer **1** (bottom). (b) Molecular packing arrangement of isomer **1** along the *a* axis, showing the intermolecular hydrogen-bonding interactions.

Structural Results. One asymmetric unit of the structure of $\mathbf{1} \cdot 2\text{H}_2\text{O}$ contains two isomers **1** and four water molecules. An ORTEP drawing of one of the isomers is shown in Figure 1a. In isomer **1**, two $[\text{Ni}(\text{CN})_4]^{2-}$ anions bridge two *cis*- $[\text{Ni}(\text{f-}rac\text{-L})]^{2+}$ in *cis*-positions to form a [2+2] type of discrete molecular square. The macrocyclic ligand **L** in isomer **1** adopts a folded *cis* conformation. The Ni(1)–N(macrocycle) distances [2.106(4)~2.187(4) Å] are close to the Ni(1)–N(cyano) distances [2.100(4) and 2.121(3) Å], and they are longer than the Ni(2)–C(cyano) distances [1.849(5)~1.881(5) Å]. The C–N(coordinated) distances of the cyano groups are close to the C–N(uncoordinated) distances (see Table 2). The two $[\text{Ni}(\text{CN})_4]^{2-}$ anions in the square are parallel, with a dihedral angle of 0.0° between the two $[\text{Ni}(\text{CN})_4]^{2-}$ planes. The molecular squares are packed along the *a* axis (Figure 1b) and combined together through

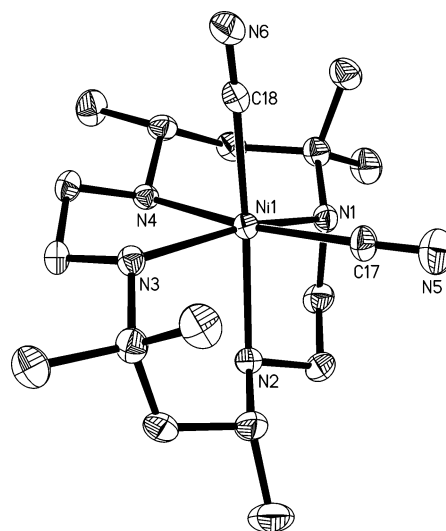


Figure 2. ORTEP drawing of the segment of isomer **2**. Thermal ellipsoids are drawn at the 30% level.

intermolecular hydrogen bonding interactions [O(1W)···N(15) = 2.765, O(1W)···N(16)^a = 2.934, O(1W)···N(12)^b = 2.910, O(2W)···N(8)^c = 2.684 Å; *a* = *x*, −*y* + 3/2, *z* + 1/2; *b* = *x*, −*y* + 3/2, *z* − 1/2; *c* = −*x* + 2, −*y* + 1, −*z*].

Compound **2** crystallizes in a chiral space group, $P2_12_12_1$, with an absolute structure parameter of 0.036. In **2**, the Ni(II) is six-coordinated with four nitrogen atoms of the folded macrocyclic ligand **L** and two carbon atoms of cyano groups in *cis* positions (Figure 2). The Ni–C distances [2.084(4) and 2.085(4) Å] are shorter than the Ni–N distances [2.167(3)~2.211(3) Å]. There is intermolecular hydrogen bonding between water molecules and terminal nitrogen atoms of the cyano groups [O(1)···N(6) = 3.036(6), O(2)···N(6) = 2.921(7), O(1)···N(5)^a = 2.973(6), O(2)···N(5)^a = 3.022(7) Å; *a* = *x* + 1, *y*, *z*].

Isomer **3** can be regarded as the result of ring-opening polymerization of isomer **1**. In isomer **3**, the nickel(II) ions show coordination environments similar to those in isomer **1** (Figure 3a), in which the macrocyclic ligands are also arranged in a folded *cis* conformation. In contrast to isomer **1**, the Ni–N(macrocycle) distances [2.121(2)~2.159(3) Å] are slightly longer than the Ni–N(cyano) distances [2.089(3) and 2.093(3) Å]. The two adjacent $[\text{Ni}(\text{CN})_4]^{2-}$ planes are almost perpendicular, with a dihedral angle of 94.1°. The two Ni(1)–N(5)–N(8) coordination planes are also twisted with a dihedral angle of 48.4°. The perpendicular $[\text{Ni}(\text{CN})_4]^{2-}$ anions alternately bridge the *cis*- $[\text{Ni}(\text{f-}rac\text{-L})]^{2+}$ cations to form a novel 1D chiral helical chain (Figure 3b). However, the adjacent 1D helical chain is constructed with the opposite chirality, rendering the crystal achiral. The two series of 1D helical chains with alternating Δ (right-handed) and Λ (left-handed) chirality are packed together along the *b* axis to form a 3D structure (Figure 3c). The water molecules are located between the Δ and Λ series of chains and form extended intermolecular hydrogen bonds (see Table 2).

Magnetic Properties. The magnetic properties of isomer **1** are shown in Figure 4a in the form of the temperature dependence of $\chi_M T$, χ_M being the molar magnetic suscepti-

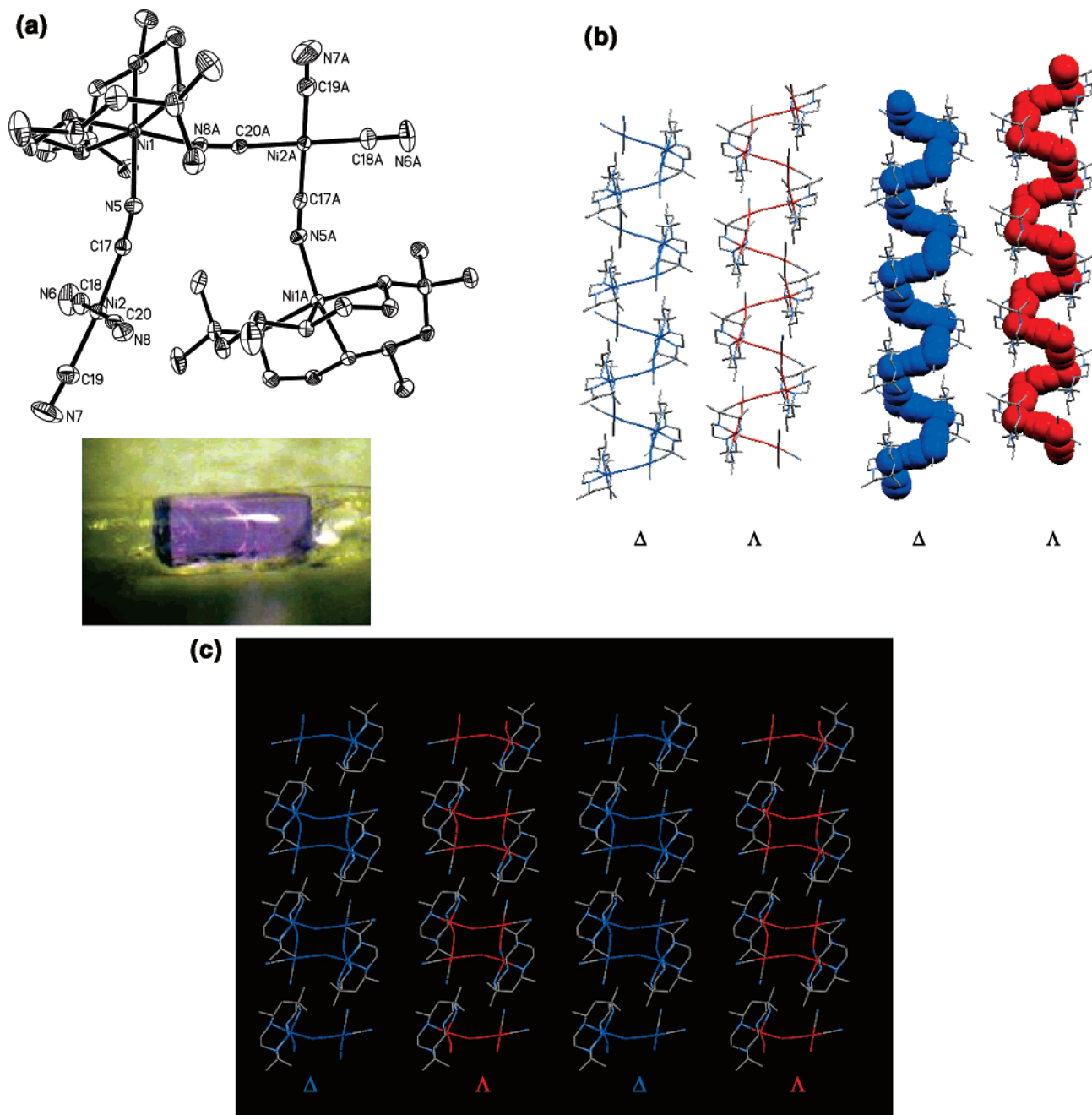


Figure 3. (a) ORTEP drawing of isomer **3** (thermal ellipsoids are drawn at the 30% level; top) and a photograph of a single crystal of isomer **3** (bottom). (b) Side view of the 1D helical chains with Δ and Λ chirality. (c) View of the 1D helical chains down the polymer axis (along the b axis), showing the alternating Δ and Λ chirality.

bility. The μ_{eff} at room temperature, $4.31 \mu_{\text{B}}$, is slightly larger than the spin-only value of $4.00 \mu_{\text{B}}$ expected for two uncoupled Ni(II) ions ($S = 1$, $g = 2.0$). With decreasing temperature, the $\chi_{\text{M}}T$ value decreases slowly from $2.32 \text{ cm}^3 \text{ mol}^{-1} \text{ K}$ at 280 K to $2.08 \text{ cm}^3 \text{ mol}^{-1} \text{ K}$ at 9.0 K, then decreases rapidly to $1.69 \text{ cm}^3 \text{ mol}^{-1} \text{ K}$ at 2.0 K. The plot of $1/\chi_{\text{M}}$ versus T in the range 2–280 K obeys the Curie–Weiss law with a small negative Weiss constant of $\Theta = -1.78 \text{ K}$. These observations suggest a weak antiferromagnetic interaction between the two six-coordinated Ni(II) ions through the bent $-\text{NC}-\text{Ni}-\text{CN}-$ bridges. The intramolecular magnetic interaction of isomer **1** can be represented with the isotropic

spin Hamiltonian¹¹ $\hat{H} = -\hat{S}_1\hat{S}_2$, and χ_{m} can be expressed as

$$\chi_{\text{M}} = \frac{2N\beta^2 g^2}{kT} \frac{\exp(J/kT) + 5 \exp(3J/kT)}{1 + 3 \exp(J/kT) + 5 \exp(3J/kT)} + \text{TIP}$$

where the symbols have their usual meaning. J is the exchange coupling parameter, and TIP represents metallic impurities.

As shown in Figure 4a, this model reproduces very well all the experimental points and leads to g , J , and TIP values

(11) Xiang, H.; Lu, T. B.; Chen, S.; Mao, Z. W.; Feng, X. L.; Yu, K. B. *Polyhedron* **2001**, *20*, 313 and references therein.

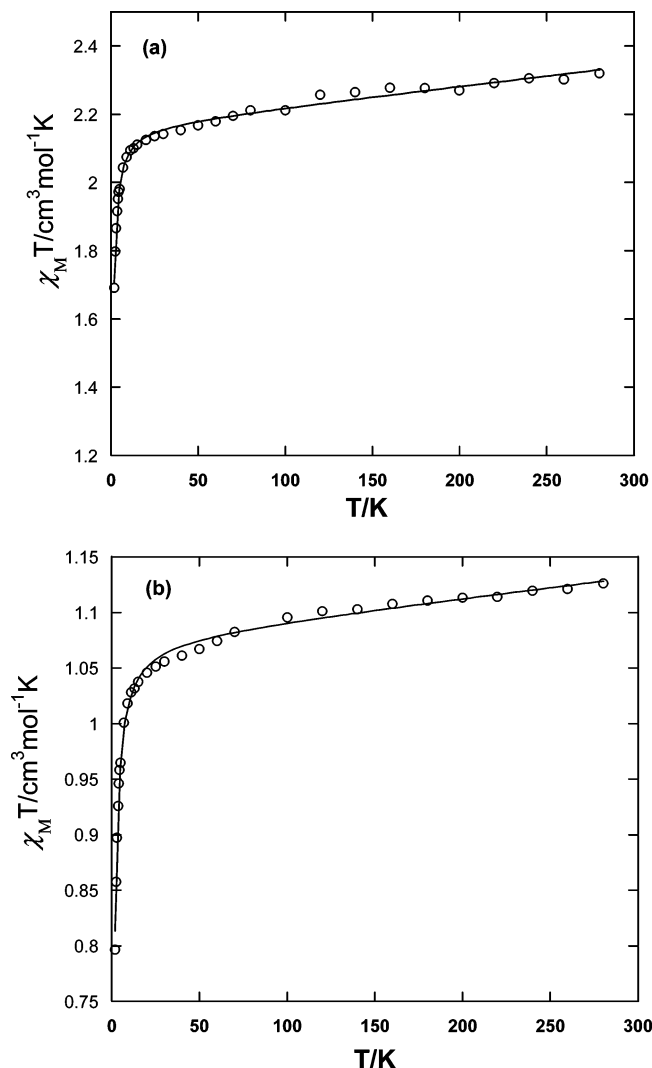


Figure 4. Temperature dependence of $\chi_M T$ vs T for isomer **1** (a) and isomer **3** (b). The solid lines are the best-fit curve.

of 2.08, -0.426 cm^{-1} , and 5.98×10^{-4} , respectively, with a correlation coefficient of 0.997 61.

Isomer **3** shows magnetic properties similar to those of isomer **1** (Figure 4b). The value of $\chi_M T$ at room temperature, $1.13 \text{ cm}^3 \text{ mol}^{-1} \text{ K}$ ($3.01 \mu_B$; if the data is calculated per $\{[\text{NiL}][\text{Ni}(\text{CN})_4]\}_2$ unit, the $\mu_{\text{eff}} = 4.26 \mu_B$), is close to the value of $1.00 \text{ cm}^3 \text{ mol}^{-1} \text{ K}$ ($2.83 \mu_B$) of an isolated Ni(II) ion ($S = 1$, $g = 2.0$) and decreases slightly with decreasing temperature to reach $1.00 \text{ cm}^3 \text{ mol}^{-1} \text{ K}$ at 7.0 K, then decreases rapidly to $0.80 \text{ cm}^3 \text{ mol}^{-1} \text{ K}$ at 2.0 K. An analysis of the magnetic data by the Curie–Weiss law reveals a weak antiferromagnetic coupling with a small negative Weiss constant of $\Theta = -1.46 \text{ K}$.

We fitted the magnetic data for **3** using Kahn's expression¹² for a 1D chain with antiferromagnetic coupling ($J < 0$):

$$\chi_{\text{chain}} = \frac{Ng^2\beta^2}{kT} \frac{2.0 + 0.0194x + 0.777x^2}{3.0 + 4.346x + 3.232x^2 + 5.834x^3} + \text{TIP}$$

with

$$x = |J|/kT$$

The least-squares fitting of all experimental points leads to J , g , and TIP values of -0.278 cm^{-1} , 2.08, and 1.89×10^{-4} , respectively, with a correlation coefficient of 0.997 57.

The J value and Weiss constant of isomer **3** (-0.278 cm^{-1} and -1.46 K , respectively) are smaller than those of isomer **1** (-0.426 cm^{-1} and -1.78 K), indicating a relatively weaker antiferromagnetic coupling through the bent $-\text{NC}-\text{Ni}-\text{CN}-$ bridges in isomer **3**. The weaker antiferromagnetic coupling in isomer **3** may be due to the twist of adjacent Ni(1)–N(5)–N(8) coordination planes, which results in less efficient antiferromagnetic coupling through the bent $-\text{NC}-\text{Ni}-\text{CN}-$ bridges.

In conclusion, the metastable compound **2** and two Ni(II) supramolecular isomers of a discrete closed molecular square, **1**, and a 1D helical chain, **3**, with alternating right- and left-handed chirality were successfully constructed. Isomer **3** can be considered to be formed by the ring-opening polymerization of the square precursor of **1**. The twisted arrangements of two adjacent $[\text{Ni}(\text{CN})_4]^{2-}$ anions lead to the formation of a 1D helical chain instead of a 1D zigzag chain. Isomer **3** can also be obtained by the conversion of **2** in a $\text{CH}_3\text{OH}/\text{CH}_3\text{CN}$ solution. In comparison with isomer **1**, isomer **3** shows a weaker antiferromagnetic coupling within the chain due to the twist of adjacent Ni(1)–N(5)–N(8) coordination planes.

Acknowledgment. This work was supported by NSFC (20371051) and NSF of Guangdong Province (04205405). We thank John F. Berry for assistance with corrections, Hui-Zhong Kou for useful suggestions on magnetic properties, and Jun-Hua Yao for assistance in running the ESI-MS spectra.

Supporting Information Available: X-ray crystallographic data for **1**·2H₂O, **2**·2H₂O, and **3**·(4.5H₂O)_n in CIF format and ESI-MS spectra of **1** and **2** (PDF). This material is available free of charge via the Internet at <http://pubs.acs.org>.

IC050626W

(12) (a) Meyer, A.; Gleizes, A.; Girerd, J.-J.; Verdager, M.; Kahn, O. *Inorg. Chem.* **1982**, *21*, 1729. (b) Kahn, O. *Molecular Magnetism*; VCH Press: New York, 1993; p 258.